



Synthesis of very highly dispersed platinum catalysts supported on carbon xerogels by the strong electrostatic adsorption method

Stéphanie Lambert^{a,*}, Nathalie Job^a, Lawrence D'Souza^b, Manuel Fernando Ribeiro Pereira^c, René Pirard^a, Benoît Heinrichs^a, José Luis Figueiredo^c, Jean-Paul Pirard^a, John R. Regalbuto^b

^a Laboratoire de Génie Chimique, B6a, Université de Liège, B-4000 Liège, Belgium

^b Chemical Engineering Department, University of Illinois at Chicago, 810 S. Clinton Street, Chicago, IL 60607, USA

^c Laboratório de Catálise e Materiais (LCM), Laboratório Associado LSRE/LCM, Departamento de Engenharia Química, Faculdade de Engenharia, Universidade do Porto, Rua Dr. Roberto Frias, 4200-465 Porto, Portugal

ARTICLE INFO

Article history:

Received 11 September 2008

Revised 24 October 2008

Accepted 27 October 2008

Available online 22 November 2008

Keywords:

Strong electrostatic adsorption

Platinum catalysts

Carbon xerogel

Aqueous sol–gel process

Benzene hydrogenation

ABSTRACT

Highly dispersed Pt/carbon xerogel catalysts are obtained by applying the “strong electrostatic adsorption” (SEA) of hexachloroplatinic acid to carbon xerogels (PZC = 9.4) and platinum tetraammine chloride to oxidized carbon xerogels (PZC = 2.4). After the reduction step, all these Pt/carbon xerogel catalysts display a very high level of metal dispersion: very small platinum particles (1.1–1.3 nm) are observed by TEM. Pt particle sizes obtained by CO chemisorption are in good agreement with TEM micrographs, which shows that the metal is accessible to reactants. These Pt/carbon xerogel catalysts are very active for the hydrogenation of benzene into cyclohexane.

© 2008 Elsevier Inc. All rights reserved.

1. Introduction

For several years, the synthesis of Pt/C fuel cell electrocatalysts has been in a great expansion. The catalytic layer of proton exchange membrane fuel cells (PEMFCs) is indeed a key element to the cell performance; in particular, the carbon pore texture as well as the platinum dispersion and crystalline structure are known to strongly influence the electrode performance [1]. Most of the air/H₂ PEMFC electrodes use platinum catalysts supported on carbon blacks, which are composed of carbon particles (10–30 μm) assembled together as aggregates. The packing of these aggregates, and therefore the pore structure of the catalytic layer, depends on the carbon black nature and on the electrode processing. Typically, at the air-fed cathode, where oxygen, proton and water transports are involved, high potential losses due to diffusion limitations offset the cell performances; this problem is compensated by increasing the metal loading, to the detriment of the cost of such devices. As detailed by Gasteiger et al. [2], the necessary reduction of platinum loading must be led in two ways: (i) improvement of the catalyst activity and efficiency, either by optimizing the metal dispersion or by using appropriate alloys and (ii) improvement of the electrode structure in order to decrease the diffusion-induced po-

tential losses. In the latter field, nanostructured carbons constitute an interesting alternative to carbon blacks.

Recently, carbon aerogels and xerogels were used to replace classical carbon supports in catalysis [3–5] and electrocatalysis [6–9] applications. These materials are obtained either by supercritical drying or evaporative drying of organic gels, followed by pyrolysis [10,11], and their pore texture is fully controllable within a wide range via the synthesis variables of the pristine gel. With regard to active carbons or carbon blacks, the advantages of carbon aerogels and xerogels are their high purity and their pore texture flexibility. For example, carbon xerogels were recently used as a Pd and Pd–Ag catalyst supports in order to eliminate diffusional limitations during a gas phase reaction [12]. In previous studies [7,8], PEMFCs cathodes were prepared from Pt catalyst supported on carbon aerogels and xerogels. While carbon blacks are constituted of aggregates connected through van der Waals bonds, carbon aerogel and xerogel powders display monolithic structures at the micrometer scale; as a consequence, the pore texture of a carbon aerogel or xerogel micromonolith remains identical in the catalytic layer of a membrane–electrode assembly [7,8]. These previous works showed that an adequate choice of the carbon pore texture could lead to a significant decrease of the diffusion-induced potential losses. However, the highly loaded (35 wt%) Pt catalysts used in these studies, and prepared by direct deposition of large metal amounts on the support, presented low metal dispersions: up to 60% of the Pt atoms constituted large particles (10–50 nm), which decreased the

* Corresponding author. Fax: +32 4366 3545.

E-mail address: stephanie.lambert@ulg.ac.be (S. Lambert).

Pt utilization ratio. In addition, the synthesis method was rather long and sophisticated. In order to increase the efficiency of carbon aerogel and xerogel supported Pt catalysts, it is thus necessary to develop a simple procedure to obtain Pt catalysts with relatively high metal loading and optimal dispersion.

Much progress in the preparation of heterogeneous catalyst has been made through the postulate of Brunelle that the adsorption of noble metal complexes onto common oxide supports was essentially coulombic in nature [13]. The hydroxyl ($-OH$) groups that populate oxide surfaces become protonated and so positively charged below a characteristic pH value, while the same hydroxyl groups become deprotonated and negatively charged above this characteristic pH value. This pH, at which the surface is neutral, is termed the point of zero charge (PZC). Brunelle explained that oxides placed in solutions at pH values below their PZC would adsorb anions such as hexachloroplatinate $[PtCl_6]^{2-}$; at pH values above their PZC, the same support would adsorb cations such as platinum tetraammine $[Pt(NH_3)_4]^{2+}$. A few years ago, Regalbuto et al. studied this adsorption process, beginning with the chloroplatinic acid (H_2PtCl_6 or CPA)/alumina system [14–17]. In this system, anionic chloride ($PtCl_6^{2-}$) and oxy-chloride ($PtCl_5(OH)^{2-}$, $PtCl_4(OH)(H_2O)^-$) complexes adsorb over a positively charged alumina surface in the low pH range. This method, called the “strong electrostatic adsorption” (SEA) method, has also extended to the platinum ammonium chloride ($Pt(NH_3)_4Cl_2$ or PTA)/silica system at high pH [18, 19], where cationic complexes ($Pt(NH_3)_4^{2+}$) adsorb over negatively charged surfaces. The latter two works especially demonstrate the practical consequence that, when strongly adsorbed at the optimal pH, the monolayer of adsorbed coordination complexes retains its high dispersion through the catalyst pretreatment process such as drying and reduction steps. Finally, the SEA method was applied to the activated carbon surfaces because controlled oxidation of a carbon surface at mild or rigorous conditions leads to a lesser or greater amount of oxygen functional groups on the surface [20–23], irreversibly altering the PZC and influencing the adsorption of Pt complexes in a way that is systematic and controllable. In a previous work on activated carbons [24], the highest-PZC active carbons adsorb the largest amount of anions $[PtCl_6]^{2-}$ and the lowest amount of cations $[Pt(NH_3)_4]^{2+}$ while the lowest-PZC active carbons adsorb the lowest amount of anions and the largest amount of cations. Pt uptakes reach a maximum with respect to pH for a given metal precursor and active carbon PZC.

The aim of the present work was to apply the same method to carbon xerogels in order to establish whether or not highly dispersed Pt catalysts can be prepared by optimizing the adsorption pH with regard to both the carbon surface chemistry and the chosen precursor. In this ambit, the PZC of the carbon xerogels, before and after oxidation treatment, was first determined. Then, the influence of PZC alteration on the control of Pt uptake, using both anionic and cationic Pt complexes, was studied. Finally, the impact of the impregnation method on the metal dispersion was checked. The final goal was to develop a simple and effective way to synthesize highly loaded and highly dispersed Pt/carbon materials that could be further used as electrocatalysts in PEM fuel cells.

2. Experimental and methods

2.1. Synthesis

2.1.1. Carbon xerogels synthesis

Four carbon xerogels with various pore textures were synthesized by the evaporative drying and pyrolysis of resorcinol-formaldehyde gels following a method described in a previous study [25]. Basically, the gel was obtained by polycondensation of resorcinol with formaldehyde in water, with NaOH as basification agent, whose role is to settle the starting pH of the pre-

cursor solution. The resorcinol/formaldehyde molar ratio, R/F , was fixed at 0.5 and the dilution ratio, D , i.e. the solvent/(resorcinol + formaldehyde) molar ratio, was chosen to be equal to 5.7. 99 g of resorcinol (Vel, 99%) were first mixed with 188 ml of deionized water in 500 ml vessels under stirring. After dissolution, the pH value was increased close to the chosen starting value with concentrated sodium hydroxide solutions (5 and 2 N). 135 ml of formaldehyde solution (37 wt% in water, stabilized with 10–15 wt% methanol) were added to the mixture, and the pH was then adjusted exactly to the value chosen by the addition of diluted sodium hydroxide solution (0.5 N). In order to cover a wide range of pore textures, the starting pH of the four solutions was adjusted to 5.50, 5.75, 6.00, and 6.25 respectively. The vessels were then sealed and heated up to 343 K for 72 h for gelling and aging. The gels obtained were then dried under vacuum according to the following procedure: the flasks were opened and put into a drying oven at 333 K, then the pressure was progressively decreased down to the minimum value (1200 Pa). This step was performed over 48 h. The samples were then kept at 423 K for 72 additional h. After drying, pyrolysis was performed at 1073 K under flowing nitrogen and following the same temperature program, as described in previous studies [4,25,26]: (i) ramp at 1.7 Kmin^{-1} to 423 K and hold for 15 min; (ii) ramp at 5 Kmin^{-1} to 673 K and hold for 60 min; (iii) ramp at 5 Kmin^{-1} to 1073 K and hold for 120 min; and (iv) cool slowly down to room temperature.

Oxidized carbon xerogels were also prepared by treating the above-obtained carbon materials with nitric acid. 20 g of each carbon xerogel were oxidized in an HNO_3 aqueous solution (5 N) for 48 h at room temperature. Afterwards, oxidized carbon xerogels were washed with deionized water until the pH of the washing solutions reached 4.5. These four samples were dried under vacuum (1200 Pa) at 298 K for 24 h, and then under helium (0.04 mmol s^{-1}) at 473 K for 1 h to release a great number of micropores. According to Figueiredo et al. [21], no surface oxygen groups are removed at 473 K.

Finally, all unoxidized and oxidized carbon xerogels were crushed and sieved between 100 and 500 μm before their use for the synthesis of Pt/carbon xerogel catalysts by the SEA method.

The four carbon supports are labeled as follows: the letter X (for “xerogel”) is followed by the initial pH of the precursor solution multiplied by 100. For example, X-550 is a carbon xerogel issued from the drying and pyrolysis of a gel prepared at an initial pH of 5.50. In the case of the corresponding oxidized carbon supports, the abbreviation “Ox” follows the names of the initial carbon xerogels (e.g. X-550-Ox).

2.1.2. Determination of the point of zero charge (PZC) of carbon xerogels

As explained in the Section 1, when using the SEA method, it is very important to know the PZC of the support, that is the pH value at which the electrical charge density on the support surface is zero. Here, the PZCs of unoxidized and oxidized carbon xerogels were determined by the method of Park and Regalbuto (equilibrium pH at high loading, EpHL) [27]: the porous solid is soaked in water solutions of various starting pHs and after stabilization, the pH is measured again. The PZC of the solid corresponds to a plateau in a plot of the final pH vs the initial pH. A critical operating variable in a such system is the total material surface area in solution, i.e. the surface loading, SL (units: $\text{m}^2\text{ l}^{-1}$). When comparing samples with different surface areas, the mass of the sample can be adjusted so as to achieve the same SL in each case. In the present study, the SL was chosen to be equal to $10^4\text{ m}^2\text{ l}^{-1}$ for all the carbon xerogels, in line with previous studies [27,28]. Therefore, before measuring the equilibrium pH, the mass of the eight carbon xerogels was adjusted so that $SL = 10^4\text{ m}^2\text{ l}^{-1}$ in 25 ml of water.

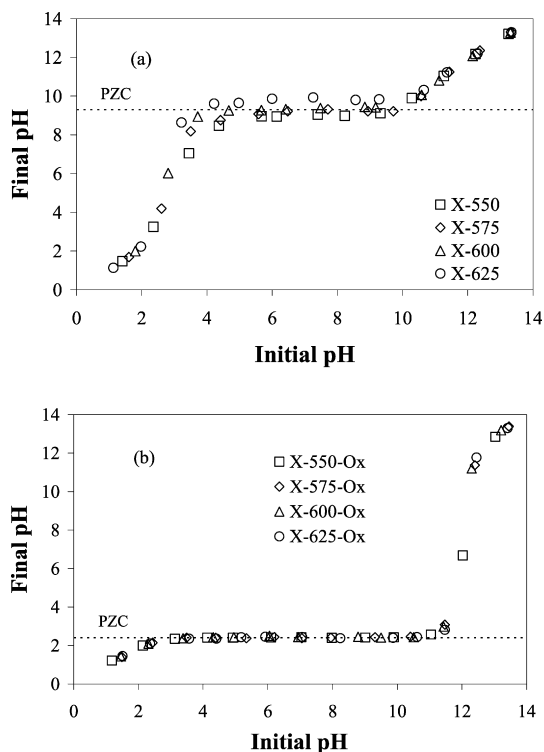


Fig. 1. PZC determination of (a) unoxidized carbon xerogels, and of (b) oxidized carbon xerogels.

Using a spear-tip semi-solid electrode (Electrode Accumet), the equilibrium pH of the eight carbon xerogels was measured over a wide range of initial pH values (from pH 1 to 13) adjusted using HCl or NaOH solutions (Fig. 1).

2.1.3. Determination of the optimal adsorption pH

In order to determine the optimal pH condition leading to maximum metal loading, adsorption experiments were conducted under various pH conditions, according to the PZC value of the supports. Chloroplatinic acid (CPA, H_2PtCl_6) (Aldrich, 99.9%) and tetraammineplatinum chloride (PTA, $\text{Pt}(\text{NH}_3)_4\text{Cl}_2$) (Aldrich, 99.9%) were used for adsorption on unoxidized and oxidized supports respectively. Aqueous solutions of CPA and PTA ($5.1 \times 10^{-3} \text{ mol l}^{-1}$) were prepared and poured into several 50-ml flasks. The pH values of all these solutions were adjusted using HCl or NaOH between pH 1 and 13 (Fig. 2).

The adsorption experiments were carried out in an excess of liquid to enable the measurement of the solution's pH and to prevent large shifts due to the "solid buffering" effect [17,24,28]. Thus before the adsorption experiments, the mass of the eight carbon xerogels was adjusted so that $\text{SL} = 10^3 \text{ m}^2 \text{ l}^{-1}$ in 25 ml of aqueous solution of CPA or PTA.

Following this, contacted slurries were placed on a rotary shaker for 1 h, after which the final pHs of these slurries were measured again (Fig. 2). Furthermore, 3–4 ml of the contacted slurries was withdrawn and filtered. The remaining concentration of Pt in the solution was determined by inductively coupled plasma (ICP) with a Perkin–Elmer Optima 2000 ICP instrument. Previous studies with activated carbons [24,28] have shown that 1 h is more than sufficient to achieve adsorption equilibrium over such surfaces. Platinum uptakes from pH 1.5 to 13 were determined from the difference in Pt concentration between the precontacted and postcontacted solutions (Fig. 2).

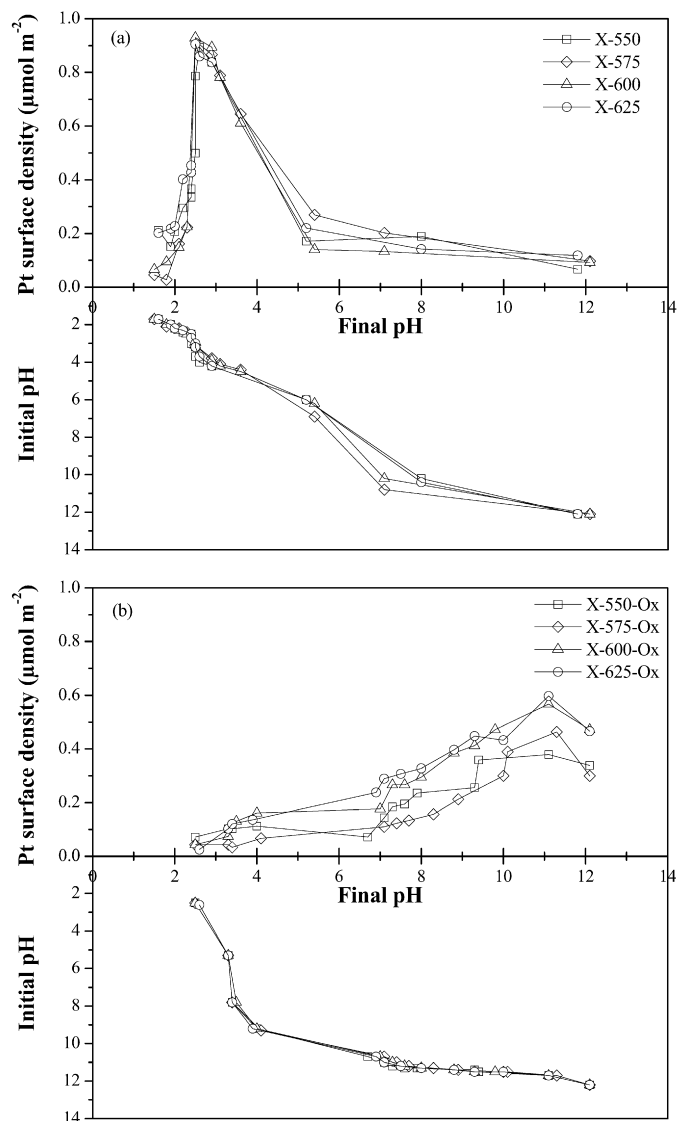


Fig. 2. (a) Final pH versus initial pH curves and CPA uptake curves of unoxidized carbon xerogels and (b) Final pH versus initial pH curves and PTA uptake curves of oxidized carbon xerogels.

2.1.4. Determination of the concentration of the minimal precursor

Before synthesizing large amounts of Pt/carbon xerogel catalysts, bearing in mind that platinum salts are very expensive, it is interesting to determine the lowest initial CPA or PTA concentration that will allow the highest level of adsorbed Pt salt on carbon xerogels to be reached after 1 h. These CPA and PTA concentrations were determined experimentally: (i) for CPA, 0.0378 g of sample X-625 was added to 25 ml of four CPA aqueous solutions with various concentrations varying from 1.3 to 10.2 mmol l^{-1} , and the pH was adjusted to between 2.5 and 3.0 (initial optimal pH for the adsorption of CPA onto unoxidized carbon xerogels—Fig. 2a). After 1 h on the rotary shaker, the pH of the four slurries was determined again: its value was the same in all the slurries, that is 2.4–2.5 (Fig. 2a); (ii) in the case of PTA, 0.0382 g of sample X-625-Ox was added to 25 ml of five PTA aqueous solutions with various concentrations varying from 1.3 to 11.8 mmol l^{-1} ; then the pH was adjusted at 11.7 (initial optimal pH for the adsorption of PTA onto oxidized carbon xerogels—Fig. 2b). Again, the pH of the slurries was measured after 1 h on the rotary shaker, and was found to be equal to 11.1–11.2 in each case (Fig. 2b). Finally, the amount of adsorbed Pt was determined from the difference in Pt concentration

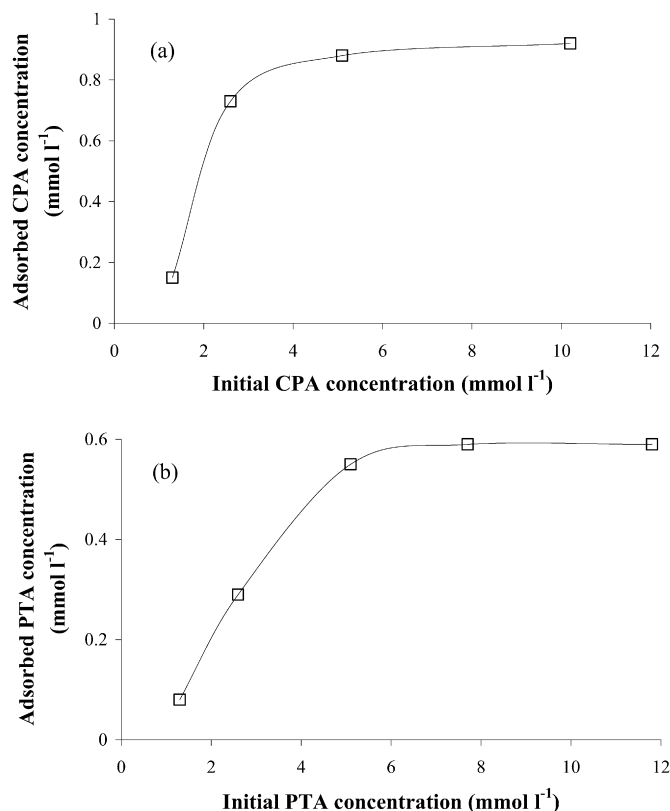


Fig. 3. Determination of the optimal initial Pt concentration for (a) sample X-625 (CPA) and (b) sample X-625-Ox (PTA).

between the precontacted and postcontacted solutions, measured by ICP (Fig. 3).

2.1.5. Synthesis of Pt/carbon xerogel catalysts

From the unoxidized carbon xerogels, 2 g of Pt/carbon xerogel catalysts were synthesized with CPA (initial concentration = 4.1 mmol l⁻¹) at SL = 10³ m² l⁻¹ and at the initial pH of between 2.5 and 3.0. The corresponding Pt catalysts are labeled as SEA-550, SEA-575, SEA-600 and SEA-625. In the case of oxidized carbon xe-

rogel, 2 g of Pt/carbon xerogel catalysts were synthesized with PTA (initial concentration = 6.0 mmol l⁻¹) at SL = 10³ m² l⁻¹ and at the initial pH of 11.7. These Pt/carbon xerogel catalysts are labeled as SEA-550-Ox, SEA-575-Ox, SEA-600-Ox and SEA-625-Ox in the sections below. Again, platinum loadings were determined from the difference between Pt concentrations in the precontacted and postcontacted solutions (Table 1). Afterwards, all Pt/carbon xerogel catalysts were dried in an oven at 393 K for 12 h. For the reduction step, Pt/carbon xerogel catalysts were heated up to 473 K under flowing H₂ (0.04 mmol s⁻¹) and were maintained at this temperature for 1 h (using the same flow).

For comparison purposes, eight Pt/carbon xerogel catalysts were prepared by dry impregnation of unoxidized and oxidized carbon xerogels with solutions of CPA (for unoxidized carbon xerogels) and PTA (for oxidized carbon xerogels). The amount of liquid was chosen to be equal to the pore volume of the supports, V_v (Table 2). The concentrations of the CPA and PTA solutions were thus adjusted so as to obtain the same platinum loading as that achieved in the eight Pt/carbon xerogel catalysts synthesized by the SEA method (Table 1). These eight Pt catalysts were labeled in the same way as the eight Pt/carbon xerogel catalysts synthesized by the SEA method, except that the abbreviation “SEA” was replaced by the abbreviation “DI.”

2.2. Characterization

Textural properties of all the samples were obtained by nitrogen adsorption–desorption isotherms and mercury porosimetry measurements. Nitrogen adsorption–desorption isotherms were measured at 77 K with a Fisons Sorptomatic 1990 after outgassing at 10⁻³ Pa for 24 h at ambient temperature. These isotherms provided the BET specific surface area, S_{BET}, the specific mesopore surface area determined by the Broekhoff–de Boer method, S_{meso}, the micropore volume calculated by the Dubinin–Radushkevich equation, V_{DUB}, the cumulative volume of pores of width between 2 and 7.5 nm determined by the Broekhoff–de Boer theory, V_{cum<7.5 nm}, and the pore volume calculated from the adsorbed volume at saturation, V_p [29]. Mercury porosimetry measurements were performed with a Pascal porosimeter thermoelectron and provided the pore volume corresponding to pores of a width >7.5 nm, V_{Hg}. In the case of macroporous samples (pore size >50 nm), the pore volume calculated from the adsorbed vol-

Table 1
Platinum loading, particle size and dispersion.

Sample	%Pt _{SEA} (wt%) ± 0.5	%Pt _{ICP} (wt%) ± 0.1	TEM		CO chemisorption		
			d _{TEM} (nm)	σ _{TEM} (nm)	n _{CO} (mmol g _{Pt} ⁻¹) ± 0.05	D _{Pt} (%) ± 5	d _{chem} (nm) ± 0.1
SEA-550	8.0	7.5	1.1	0.1	2.75	85	1.3
SEA-575	8.0	– ^a	1.2	0.1	– ^a	– ^a	– ^a
SEA-600	10.0	– ^a	1.2	0.1	2.55	80	1.4
SEA-625	9.0	9.2	1.1	0.1	2.70	85	1.3
SEA-550-Ox	1.0	1.2	1.2	0.2	2.70	85	1.3
SEA-575-Ox	2.0	– ^a	1.2	0.1	– ^a	– ^a	– ^a
SEA-600-Ox	4.0	– ^a	1.3	0.2	2.45	75	1.5
SEA-625-Ox	5.0	4.0	1.3	0.1	2.40	75	1.5
DI-550	8.0	8.0	1.1	0.1	– ^a	– ^a	– ^a
DI-575	8.0	– ^a	1.3	0.1	– ^a	– ^a	– ^a
DI-600	9.0	– ^a	1.1	0.1	– ^a	– ^a	– ^a
DI-625	8.0	7.3	1.2	0.1	2.65	85	1.3
DI-550-Ox	1.0	0.7	4 to 25	–	– ^a	– ^a	– ^a
DI-575-Ox	2.0	– ^a	4 to 25	–	– ^a	– ^a	– ^a
DI-600-Ox	4.0	– ^a	4 to 25	–	– ^a	– ^a	– ^a
DI-625-Ox	5.0	4.1	4 to 25	–	0.05	<5	>20

%Pt_{SEA}: platinum loading determined as the difference in Pt concentrations in the precontacted and postcontacted solutions; %Pt_{ICP}: platinum loading determined by ICP-AES on the final Pt/C catalysts after drying and reduction; d_{TEM}: mean diameter of platinum particles measured by TEM; σ_{TEM}: standard deviation associated with d_{TEM}; n_{CO}: amount of chemisorbed CO per Pt unit mass; D_{Pt}: platinum dispersion measured by chemisorption; d_{chem}: mean platinum diameter derived from dispersion D.

^a Not measured.

Table 2
Textural properties of carbon xerogels.

Sample	S_{BET} (m^2/g) ± 5	S_{meso} (m^2/g) ± 5	$d_{p,\text{max}}$ (nm) ± 1	V_p (cm^3/g) ± 0.1	V_{DUB} (cm^3/g) ± 0.01	$V_{\text{cum}<7.5 \text{ nm}}$ (cm^3/g) ± 0.01	V_{Hg} (cm^3/g) ± 0.1	V_v (cm^3/g) ± 0.1
X-550	635	110	90	0.8	0.25	0.04	2.8	3.1
X-575	660	150	68	0.9	0.25	0.05	2.5	2.8
X-600	660	245	32	1.0	0.24	0.09	1.9	2.2
X-625	660	300	18	1.1	0.25	0.14	1.3	1.7
X-550-Ox	625	90	93	0.9	0.20	0.04	2.7	2.9
X-575-Ox	640	145	72	1.0	0.21	0.04	2.5	2.7
X-600-Ox	640	240	35	1.0	0.20	0.09	1.7	2.0
X-625-Ox	655	285	20	1.0	0.20	0.13	1.4	1.7

S_{BET} : specific surface area obtained by BET method; S_{meso} : specific mesopore surface area obtained by the Broekhoff–de Boer method; $d_{p,\text{max}}$: the pore diameter limit under which smaller pores represent 95% of the total pore volume; V_p : total pore volume calculated from the adsorbed volume at saturation; V_{DUB} : micropore volume calculated by the Dubinin–Radushkevich equation; $V_{\text{cum}<7.5 \text{ nm}}$: cumulative volume of pores of diameter between 2 and 7.5 nm determined by Broekhoff–de Boer theory; V_{Hg} : specific pore volume measured by mercury porosimetry; V_v : pore volume obtained by addition of V_{DUB} , $V_{\text{cum}<7.5 \text{ nm}}$ and V_{Hg} .

ume at saturation is usually very imprecise or incomplete; the total void volume, V_v , was calculated from the combination of nitrogen adsorption–desorption and mercury porosimetry measurements [30]:

$$V_v = V_{\text{DUB}} + V_{\text{cum}<7.5 \text{ nm}} + V_{\text{Hg}} \quad (1)$$

In the case of the micro/mesoporous samples, the maximum pore diameter, $d_{p,\text{max}}$, i.e. the pore diameter limit under which smaller pores represent 95% of the total pore volume, was deduced from pore size distribution provided by the Broekhoff–de Boer method, assuming an open cylinder geometry [29]. In the case of macroporous samples, the pore size distribution must be deduced from mercury porosimetry data. Because macroporous samples undergo intrusion only during an increase in mercury pressure, as already observed in other studies [4,25,26], the pore size distribution was calculated here following Washburn's theory [31].

The actual platinum content of the catalysts after adsorption, drying and reduction was measured by inductively coupled plasma–atomic emission spectrometry (ICP–AES), using an Iris advantage Thermo Jarrel Ash device. For analysis, the Pt solution was prepared as follows: first, 0.1 g of catalyst were digested by 20 ml of H_2SO_4 (95 wt%) and 10 ml of HNO_3 (70 wt%), and the resulting solution was then heated at 573 K until clear (after about 16 h). After complete dissolution of the carbon support and evaporation, 3 ml of HNO_3 (70 wt%) and 9 ml of HCl (38 wt%) were added. The obtained solution was transferred into a 100-ml calibrated flask, which was finally filled with deionized water.

The metal particles were examined by transmission electron microscopy (TEM) and CO chemisorption. TEM measurements were performed on the reduced catalyst samples. A few mg of catalyst sample were dispersed in isopropanol and were sonicated for 10 min. A drop of the suspension was then placed onto a carbon-coated copper grid purchased from SPI supplies, USA. Z-contrast Imaging was carried out by using an electron microscope (JEM-2010F FaSTEMm FEI) manufactured by JEOL, USA operated at 200 kV and with an extracting voltage of 4500 V. For statistical purposes, around 400 Pt particles were considered for the particle size distribution and the average particle size.

A volumetric static method was used for CO chemisorption [32]. Measurements were obtained on a Fisons Sorptomatic 1990 equipped with a turbomolecular vacuum pump that allows a high vacuum of 10^{-3} Pa. The non-reduced catalyst was first reduced *in situ* under hydrogen flow (0.04 mmol s^{-1}); the samples were heated from 298 to 473 K at a rate of 5 K min^{-1} and were kept at 473 K for 1 h. Afterwards, the samples were outgassed under vacuum at 463 K for 1 h. A double adsorption method was used: (i) a first adsorption isotherm, which includes both physisorption and chemisorption, was determined; (ii) then after a

2 h outgassing at 303 K, a second isotherm, which includes physisorption only, was measured. Both isotherms were determined in the pressure range of 10^{-8} to 2×10^{-1} kPa. The difference between the first and second isotherms provided the CO chemisorption isotherm.

2.3. Catalytic experiments: Benzene hydrogenation

Samples SEA-550, SEA-625, SEA-550-Ox and SEA-625-Ox were tested for the hydrogenation of benzene at atmospheric pressure.

The catalysts were first crushed and sieved again between 100 and 200 μm . Due to the fact that benzene conversion is very high on highly loaded Pt/carbon xerogel catalysts, the amount of catalyst used inside the reactor was too low to form a complete catalytic bed. To solve this problem, Pt/carbon xerogel catalysts were diluted with their original support to prepare 1 wt% Pt/carbon xerogel catalysts. Afterwards, 0.05 g of non-reduced diluted catalyst was loaded into the reactor, an autoclave Engineers' BTRS. Before the reaction, the catalyst was reduced *in situ* under H_2 (0.04 mmol s^{-1}) at 473 K for 1 h.

The C_6H_6 flow rate, controlled by a set of saturators, was $0.002 \text{ mmol s}^{-1}$. The $\text{H}_2/\text{C}_6\text{H}_6$ molar ratio was fixed at 11. All gas flows were adjusted by Bronkhorst mass flow controllers. The reactor was enclosed in a convection oven with the temperature controlled and programmed to within 0.1 K using a thermocouple located inside the reactor envelope and a PID controller. The temperature of the catalyst was also measured by a second thermocouple located just above the sample because benzene hydrogenation is highly exothermic [33]. The feed and the product streams were analyzed on-line by a gas chromatograph equipped with a flame ionization detector.

Each catalytic test started at 393 K. This temperature level was maintained until a quasi-stationary state was observed (i.e., after about 2 h). Then if the benzene conversion was <50%, the temperature was increased from 393 to 423 K. By contrast, if the conversion was >50%, the temperature was decreased from 393 K to 353 K. The reactor was kept for 30 min at each temperature step; in each case, a quasi-stationary state was observed.

The activity of the catalysts was calculated as the amount of benzene (mmol) converted into cyclohexane per gram of Pt and per second. Because this reaction is structure-insensitive on Pt-based catalysts supported on activated carbon [34–36], the activity of the catalyst is directly linked to the number of accessible metal atoms. Consequently, catalytic activity is an indirect measurement of metal dispersion, defined as the ratio between the number of surface Pt atoms and the total number of Pt atoms in the catalyst. Finally the activation energy of the reaction catalyzed by Pt was determined from measurements performed at various temperatures.

3. Results

3.1. PZC of carbon xerogels and determination of Pt uptakes

The PZCs of unoxidized and oxidized carbon xerogels are shown in Figs. 1a and 1b respectively. These curves clearly show a plateau for both types of support: the PZC value equals 9.4 in the case of unoxidized carbon xerogels, and is equal to 2.4 when the supports are oxidized.

Fig. 2 shows the Pt uptake curves: the Pt surface density, defined as the amount of Pt per m^2 of the support, is plotted against the final pH value of the slurries after 1 h on the rotary shaker. In Fig. 2a, a sharp maximum is observed in the narrow final pH range of 2.4–2.5 (initial pH range between 2.5 and 3.3 for CPA solutions). At the adsorption maximum of CPA, i.e. in the 'strong adsorption' condition, the uptake is quite similar for all the unoxidized samples, that is about $0.91 \mu\text{mol m}^{-2}$, which corresponds to a Pt loading, defined as the percentage of the Pt mass per the total mass of the catalyst, of about 11.6 wt%. In Fig. 2b, the uptake curves display a maximum for each oxidized xerogel in the pH range of 11.1–11.2. (initial pH 11.7 for PTA solutions). Depending on the support, the uptake varies from $0.60 \mu\text{mol m}^{-2}$ (X-625-Ox) to $0.38 \mu\text{mol m}^{-2}$ (X-550-Ox), that is 7.7 to 4.6 wt%.

The lowest initial CPA or PTA concentration that will allow the highest level of adsorbed Pt salt to be reached on carbon xerogels was determined from the adsorption curves obtained at the optimal pH for various Pt precursor concentrations. These curves are presented in Fig. 3a for CPA adsorbed on sample X-625, and in Fig. 3b for PTA adsorbed on sample X-625-Ox. The Pt uptake shows that increasing the Pt concentration beyond 4.1 and 6.0 mmol l^{-1} in the case of CPA or PTA precursors, respectively, does not lead to the adsorption of larger amounts of Pt complex. As a consequence, for the synthesis of Pt/carbon xerogel catalysts, the initial Pt concentration of CPA and PTA solutions was chosen to be equal to 4.1 and 6.0 mmol l^{-1} respectively.

3.2. Textural properties of carbon xerogels and Pt/carbon xerogel catalysts

The textural properties of unoxidized and oxidized carbon xerogels are shown in Table 2. In agreement with previous studies [25, 26], the texture of unoxidized carbon xerogels greatly varies with the initial pH of the resorcinol–formaldehyde solution: when the synthesis initial pH increases from 5.50 to 6.25, the total pore volume, V_v , decreases from 3.1 to $1.7 \text{ cm}^3 \text{ g}^{-1}$, and the mesopore surface area, S_{meso} , increases from 110 to $300 \text{ m}^2 \text{ g}^{-1}$. The increase of S_{meso} is due to the decrease of the meso/macropore size, $d_{p,\text{max}}$, from 90 to 18 nm. Similar trends are observed for the oxidized series: when the initial pH is increased from 5.50 to 6.25, V_v decreases from 2.9 to $1.7 \text{ cm}^3 \text{ g}^{-1}$, while S_{meso} increases from 90 to $285 \text{ m}^2 \text{ g}^{-1}$. The increase of S_{meso} is also due to the decrease of the meso/macropore size, $d_{p,\text{max}}$, from 93 to 20 nm. So the oxidation step of carbon xerogels does not change the size of the mesopores. Indeed, as the standard deviation associated with $d_{p,\text{max}}$ is about $\pm 1 \text{ nm}$, a variation from 18 to 20 nm is not significant.

After platinum adsorption by the SEA method, drying and reduction steps, the textural characteristics of all Pt/carbon xerogel catalysts vary with regards to those of the original supports. Indeed, the specific surface area, S_{BET} , and the micropore volume, V_{DUB} , decrease significantly compared to the S_{BET} and V_{DUB} of corresponding carbon xerogels used as supports for Pt/carbon xerogel catalysts: for instance, for samples X-550 and SEA-550, S_{BET} and V_{DUB} decrease respectively from 635 and $0.25 \text{ cm}^3 \text{ g}^{-1}$ before Pt adsorption to 500 and $0.22 \text{ cm}^3 \text{ g}^{-1}$ after Pt adsorption. Again for samples X-575-Ox and SEA-575-Ox, S_{BET} and V_{DUB} decrease respectively from 640 $\text{m}^2 \text{ g}^{-1}$ and $0.21 \text{ cm}^3 \text{ g}^{-1}$ before Pt adsorption

to 525 and $0.18 \text{ cm}^3 \text{ g}^{-1}$ after Pt adsorption. Moreover, for samples X-600 and SEA-600, X-625 and SEA-625, X-600-Ox and SEA-600-Ox, X-625-Ox and SEA-625-Ox, the mesopore surface area, S_{meso} , decreases too: from 300 to $250 \text{ m}^2 \text{ g}^{-1}$ for samples X-625 and SEA-625, and from 240 to $195 \text{ m}^2 \text{ g}^{-1}$ for samples X-600-Ox and SEA-600-Ox. By contrast, S_{meso} does not change much in the case of supports with large pore sizes: for instance, $S_{\text{meso}} = 110 \text{ m}^2 \text{ g}^{-1}$ for samples X-550 and SEA-550 and $S_{\text{meso}} = 150 \text{ m}^2 \text{ g}^{-1}$ for samples X-550 and SEA-575-Ox before and after Pt adsorption. These findings indicate that platinum deposition affects micropores and small mesopores only, as already observed in [37] in the case of Pt/carbon xerogel catalysts prepared by impregnation.

3.3. Platinum loading in Pt/carbon xerogel catalysts

Platinum loadings were determined by ICP-AES on the final Pt/carbon xerogel catalysts after drying and reduction ($\%Pt_{\text{ICP}}$) in order to check whether the platinum loadings calculated from the difference between Pt concentrations in the precontacted and post-contacted solutions ($\%Pt_{\text{SEA}}$) were correct (Table 1). These results show that Pt loadings determined by both methods are quite similar.

The Pt loadings of samples SEA-550, SEA-575, SEA-600 and SEA-625 obtained from the solution concentration differences, $\%Pt_{\text{SEA}}$, range from 8 to 10 wt%, which shows that the amount of adsorbed CPA is similar whatever the support, although the increase of mesopore surface seems to slightly favor adsorption. This result is in good agreement with Fig. 2a, in which at the adsorption maximum of CPA (final pH range of 2.4–2.5), the Pt uptake is quite similar for all unoxidized samples: $0.91 \mu\text{mol m}^{-2}$, which corresponds to a Pt loading of about 11.6 wt%. For samples issued from oxidized supports, SEA-550-Ox, SEA-575-Ox, SEA-600-Ox and SEA-625-Ox, $\%Pt_{\text{SEA}}$ ranges from 1.0 to 5.0 wt% (Table 1); this is in good agreement with Fig. 2b in which the amount of adsorbed PTA increases from sample X-550-Ox to sample X-625-Ox. Nevertheless, the amounts of adsorbed PTA on little amounts of oxidized carbon xerogels (about 0.038 g of oxidized carbon xerogels were used to establish Fig. 2b) are proportionally higher (Pt loadings range from 4.6 wt% for X-550-Ox to 7.7 wt% for X-625-Ox) than the amounts of Pt salts adsorbed on greater amounts of oxidized carbon xerogels (2 g of each oxidized carbon xerogel were used to synthesize samples SEA-550-Ox, SEA-575-Ox, SEA-600-Ox and SEA-625-Ox with Pt loadings from 1.0 to 5.0 wt% Table 1), assuming diffusional limitations.

Concerning the increase of Pt loadings from sample X-550-Ox to sample X-625-Ox (Fig. 2b), assuming that the number and the nature of surface oxygen groups are similar for all oxidized carbon xerogels, since their total material surface in solution was the same ($SL = 10^3 \text{ m}^2 \text{ l}^{-1}$) and since their PZC is identical, the only difference between the four samples is the surface distribution between micro-, meso-, and macropores. Indeed, S_{meso} increases from 90 to $285 \text{ m}^2 \text{ g}^{-1}$ when the synthesis pH of the pristine gel increases from 5.50 to 6.25, due to the decrease of the pore size (Table 2). Fig. 4 shows that, in the case of oxidized supports, the amount of adsorbed PTA, and thus the Pt weight loading increases linearly with S_{meso} .

3.4. Platinum dispersion in Pt/carbon xerogel catalysts

Table 1 shows the platinum particle sizes determined by TEM and CO chemisorption measurements.

TEM micrographs show that, in all Pt/carbon xerogel catalysts synthesized by the SEA method, the size of the platinum particles is quite homogeneous, and is about 1.2 nm (Figs. 5a and 5b). In order to compare the Pt dispersion obtained using the SEA method on unoxidized and oxidized carbon xerogels with that resulting

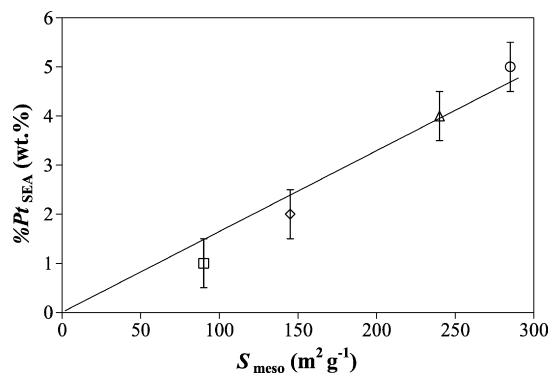


Fig. 4. Platinum weight loading as a function of the total mesoporous surface area, S_{meso} , of oxidized carbon xerogels for samples SEA-550-Ox (□), SEA-575-Ox (◇), SEA-600-Ox (△) and SEA-625-Ox (○). Adsorption of PTA (6.0 mmol l^{-1}) with an initial pH = 11.7.

from the classical dry impregnation (DI) method on the same supports, micrographs of catalysts synthesized by the DI method are also shown in Figs. 5c and 5d. Concerning Pt/carbon xerogel catalysts synthesized with CPA using either the SEA method (Fig. 5a) or the DI method (Fig. 5c), all the samples are very highly dispersed (Table 2). By contrast, Pt/carbon xerogel catalysts synthesized with PTA using the SEA method are very highly dispersed (Fig. 5b), while the same samples synthesized with PTA using the DI method present very large platinum particles from 5 to 25 nm (Fig. 5d).

From CO chemisorption measurements on Pt/carbon xerogel catalysts synthesized with the SEA method, the amount of chemisorbed CO per Pt unit mass, n_{CO} , ranges from 2.40 to 2.75 $\text{mmol g}_{\text{Pt}}^{-1}$ (Table 1). From the adsorbed amount of CO, one can calculate the platinum dispersion, D_{Pt} , i.e. the ratio between the number of Pt atoms located at the surface of the metal particles and the total number of Pt atoms in the catalyst, and the mean diameter of Pt crystallites, d_{chem} , as explained in [37]. Following

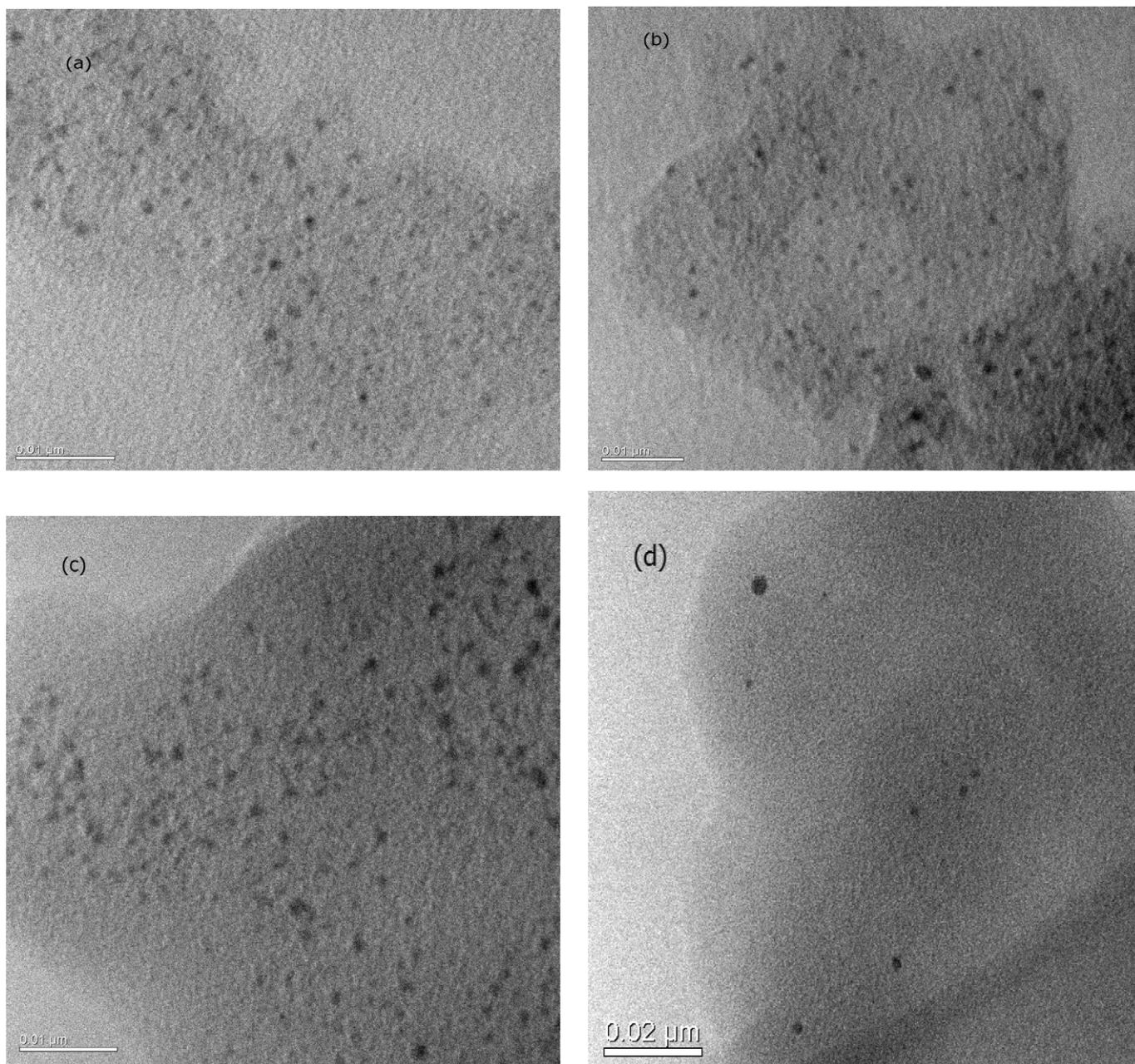


Fig. 5. STEM micrographs of samples: (a) SEA-600, (b) SEA-625-Ox, (c) DI-600, and (d) DI-625-Ox.

Table 3
Catalytic test results.

Sample	$r_{\text{ben}} \text{ (mmol g}_{\text{Pt}}^{-1} \text{ s}^{-1}) \pm 0.05$						
	353 K	363 K	383 K	393 K	403 K	413 K	423 K
SEA-550	– ^a	– ^a	– ^a	1.15	1.60	2.05	2.85
SEA-625	– ^a	– ^a	– ^a	1.05	1.50	1.90	2.50
SEA-550-Ox	1.00	1.65	2.25	2.75	– ^a	– ^a	– ^a
SEA-625-Ox	0.60	0.90	2.10	2.30	– ^a	– ^a	– ^a

r_{ben} : apparent reaction rate for benzene hydrogenation per Pt mass unit.

^a Not measured.

previous studies conducted on highly dispersed Pt catalysts [37, 38], the chemisorption mean stoichiometry $X_{\text{Pt-CO}}$, that is, the mean number of Pt atoms on which one CO molecule is adsorbed, was chosen equal to 1.61. Values of D_{Pt} and d_{chem} are given in Table 1. For all samples, one has to note the agreement between TEM and chemisorption, assuming that all the Pt atoms located at the surface of the metal particles are accessible to CO.

3.5. Catalytic activity of Pt/carbon xerogel catalysts

Catalytic test results are presented in Table 3. Benzene hydrogenation on Pt/carbon xerogel catalysts resulted in very high conversion ratios, even with low amounts of diluted catalyst (0.05 g with Pt loading = 1 wt%). The apparent reaction rate, r_{ben} , was calculated at each temperature for each catalyst, taking into account an integral isothermal reactor working in a stationary state and a first-order reaction, $r_{\text{ben}} = k[\text{C}_6\text{H}_6]$ [39]. Indeed, for these catalytic tests, the concentration of hydrogen is always much greater than the concentration of benzene ($[\text{H}_2]/[\text{C}_6\text{H}_6] = 11$). Thus, because the hydrogen partial pressure is essentially constant during the reaction, the rate observed depends only on the concentration of benzene:

$$r_{\text{ben}} = -\frac{F_{\text{ben}}}{W} \ln(1 - f), \quad (2)$$

where F_{ben} is the benzene flowrate at the inlet of the reactor (mmol s^{-1}), W is the Pt mass inside the reactor (g_{Pt}), and f is the conversion of benzene into cyclohexane.

The reaction rate observed in the present study is an apparent reaction rate: it equals the intrinsic reaction rate when no diffusional limitation occurs and when the reactor is differential only. Following the method used in previous studies [12,37], the Weisz modulus, which compares the reaction rate to the diffusion rate, was calculated to determine the importance of diffusional limitations. In all cases, the Weisz modulus was $\ll 1$, indicating that the Pt/carbon xerogel catalysts were operating in a chemical regime; the effect of the diffusion of reactants on the observed kinetics was negligible.

At 393 K, r_{ben} is equal to 1.15 and 1.05 $\text{mmol g}_{\text{Pt}}^{-1} \text{ s}^{-1}$ for samples SEA-550 and SEA-625 respectively, and r_{ben} is equal to 2.75 and 2.30 $\text{mmol g}_{\text{Pt}}^{-1} \text{ s}^{-1}$ for samples SEA-550-Ox and SEA-625-Ox respectively. The values of samples SEA-550 and SEA-625 are very similar to those presented in a previous study [37]. Nevertheless, Pt/carbon xerogel catalysts synthesized from oxidized carbon xerogels present higher values for r_{ben} .

Considering an integral isotherm reactor working in a stationary state and a first-order reaction, the relationship between the conversion, f , and the apparent activation energy of the reaction, E_a , can be written as in [39]:

$$\ln(\ln(1/(1 - f))) = \ln C - (E_a/RT), \quad (3)$$

where C is a constant, R is the perfect gas constant, and T is the temperature. The apparent activation energy for benzene hydrogenation on Pt was calculated from experimental data obtained at 393, 403, 413 and 423 K for samples SEA-550 and SEA-625, and at

353, 363, 383 and 393 K for samples SEA-550-Ox and SEA-625-Ox. E_a was found to range from 38 to 55 kJ mol^{-1} , in agreement with values reported in the literature (30–70 kJ mol^{-1} [37,38]).

4. Discussion

The PZC of carbons can be changed irreversibly by oxidizing the surface. In addition, in previous studies [22,24], it has been demonstrated that the Pt anion and cation uptakes can be modified on this basis. In the present study, the main difference between unoxidized and oxidized carbon xerogels is the number of acidic groups on the surface. Concerning unoxidized carbon xerogels, their PZC equals 9.4 (Fig. 1a), which indicates that these carbon surfaces initially contain a very low number of acidic groups. Indeed, the PZC of a carbon seems to be determined mainly by the concentration of the surface acid sites: the higher the number of acidic groups on a carbon surface, the lower its PZC [22]. When carbon xerogels are oxidized with 5 mol l^{-1} nitric acid for 48 h at room temperature, their PZC decreases to 2.4 (Fig. 1b), as a consequence of the increase of the number of their acidic surface sites, as explained extensively in previous studies [22,40].

In contrast to silica and alumina [24], carbon xerogels of varying PZC differ markedly in their capacity to adsorb Pt anion and cation complexes (Fig. 2). In Fig. 2a, the uptake of CPA adsorption on unoxidized carbon xerogels (PZC = 9.4) versus final pH shows a sharp maximum in the narrow pH range of 2.4–2.5. At the maximum adsorption of CPA, i.e. the ‘strong adsorption’ condition, the uptake is quite similar for all unoxidized samples, about 0.91 $\mu\text{mol m}^{-2}$, which corresponds to a Pt loading of about 11.6 wt%. It is for this reason that, in Table 1, the platinum loadings, $\%Pt_{\text{SEA}}$, are very similar for samples SEA-550, SEA-575, SEA-600 and SEA-625, with Pt loadings from 8.0 to 10.0 wt%. In contrast, in Fig. 2b, the uptake curve displays a maximum for each oxidized xerogel in the pH range of 11.1–11.2. Depending on the support, the maximum uptake varies from 0.38 (X-550-Ox) to 0.60 $\mu\text{mol m}^{-2}$ (X-625-Ox). Fig. 4 shows that, in the case of oxidized supports and at an initial pH 11.7 (to obtain a final pH 11.1–11.2 after mixing and stirring for 1 h; Fig. 2b), the amount of adsorbed PTA, and thus the Pt weight loading increases linearly with S_{meso} , this latter parameter increasing from 90 $\text{m}^2 \text{g}^{-1}$ for sample X-550-Ox to 285 $\text{m}^2 \text{g}^{-1}$ for sample X-625-Ox (Table 2). These results can be explained by the fact that it is not possible for the large Pt ammine complexes, which are believed to retain two hydration sheaths and the size of which is estimated equal to 1.5 nm [28,41], to penetrate inside the micropores of carbon xerogels, the size of which has been calculated to be equal to 0.8 nm [25]. Indeed, in previous studies concerning silica, alumina and active carbons [16,24], it has been explained that the maximum Pt uptake of both CPA and PTA complexes appears to be dictated by a steric maximum, which can be calculated as a closely packed monolayer of complexes that retain either one hydration sheath in the case of the anionic chloride complexes (their size has been estimated to be equal to 0.6 nm [16,28]), or two sheaths in the case of the cationic ammine complexes (their size has been estimated to be equal to 1.5 nm [28,41]). Thus for microporous supports, it is very difficult to adsorb cationic ammine complexes because their steric volume is too high compared to the size of micropores in the support. In this case, the ammine complex adsorbs at the surface of the mesopores and, as a consequence, the Pt uptake increases linearly with the mesopore surface (Fig. 4). Therefore the present study shows again how carbon xerogels can be engineered to overcome the steric hindrance limitation with PTA.

The trends in anionic and cationic Pt adsorption on unoxidized and oxidized carbon xerogels seen in the present study are consistent with the adsorption of CPA or PTA on carbon blacks and activated carbons [20,22,23,42]. Indeed, surface acidic groups (and

correspondingly low PZCs) have been shown to favor the anchoring of $[\text{Pt}(\text{NH}_3)_4]^{2-}$ on carbon blacks, whereas less severe or no oxidation (and correspondingly high PZCs) leads to a greater uptake of anionic Pt complexes onto various forms of carbons. Therefore the results presented in the present study indicate that: (i) the Pt complex (anionic or cationic) must be chosen according to the PZC of the given carbon xerogel support; (ii) an optimal pH, at which the metal complex–support interactions are the strongest and the Pt uptake is the highest, exists for each carbon xerogel/Pt complex pair, and that the optimal pH depends on the carbon xerogel/Pt complex pair selection (Fig. 2).

As explained in previous studies dealing with the preparation of Pt/active charcoal catalysts by impregnation, metal dispersion essentially depends on two parameters: the pore texture of the support and its surface composition [43–45]. On the one hand, the pore texture mostly impacts the contact between the carbon surface and the solution containing the precursor. In this respect, carbon xerogels seem more favorable to homogeneous carbon–solution contact due to the broad size distribution of meso- and macropores (the total pore volume is $>1.7 \text{ cm}^3 \text{ g}^{-1}$ in Table 2) and their pore texture homogeneity [25,26]. The pore texture of active charcoals is usually much less homogeneous than that of carbon xerogels and the volume of the large pores (meso- and macropores) is low: as a consequence, the carbon inner surface, mostly related to the microporosity, is not easily reached by the solvent, and thus by the metal precursor. On the other hand, the surface composition determines not only the interactions between the support and the precursor of the species to be deposited, but also the interactions between the support and the solvent. For instance, due to the high pyrolysis temperature, active charcoals are usually hydrophobic [43], and further oxidation is often necessary to increase their surface acidic group content and the water–carbon affinity. Note that, in the case of activated charcoals, surface acidic groups seem to have a negative effect on platinum dispersion after reduction [22,43]: this is attributed to a delocalization of the aromatic cycles π -electrons of the carbon, which are responsible for the anchoring of the reduced metal particles, by the oxygen of the acidic surface groups. By contrast, carbon xerogels are very hydrophilic after pyrolysis, despite their low acidic group content [25]. Indeed, a carbon xerogel prepared by pyrolysis at 1073 K absorbs an amount of water corresponding to 95% of its pore volume within a few minutes, whatever the carbon texture. As a consequence, carbon xerogels should then lead more easily to a good metal dispersion than active charcoals.

In the present study, Pt/carbon xerogel catalysts synthesized with the use of dilute CPA aqueous solutions by both the SEA (samples SEA-550, SEA-575, SEA-600, SEA-625) and the DI (samples DI-550, DI-575, DI-600, DI-625) methods present very high Pt dispersion as a consequence of very small Pt particles (1.1–1.3 nm). These two methods give very similar results because the pH used in the SEA method for the strong electrostatic adsorption of CPA (pH 2.5) is very close to the pH value of CPA solutions (pH 1.9) after the dissolution of H_2PtCl_6 salt in water, used for the DI impregnation.

By contrast, Pt catalysts supported on oxidized carbon xerogels present much higher dispersion values when the SEA method is used instead of the classical Dry Impregnation technique. Indeed, while the Pt particle size ranges from 4 to 25 nm for samples DI-550-Ox, DI-575-Ox, DI-600-Ox and DI-625-Ox (Table 1), d_{STEM} does not exceed 1.2 nm in the case of samples SEA-550-Ox, SEA-575-Ox, SEA-600-Ox and SEA-625-Ox. In this particular case, the SEA method provides the best solution for obtaining very highly dispersed platinum catalysts from an oxidized carbon support, i.e. the use of a cationic Pt complex and the pH optimization during the impregnation step. Indeed, in samples DI-550-Ox, DI-575-Ox, DI-600-Ox and DI-625-Ox, the presence of a large number of acidic

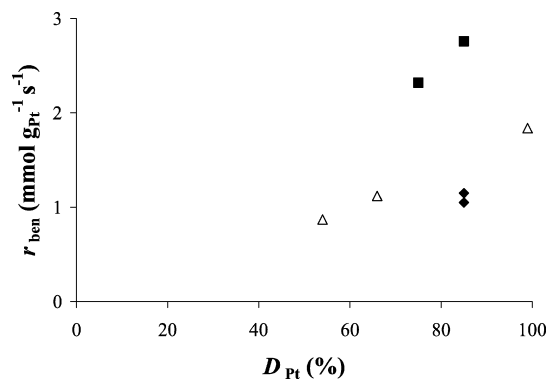


Fig. 6. Relationship at 393 K between the apparent reaction rate, r_{ben} , expressed by unit mass of Pt, and the platinum dispersion, D_{Pt} for unoxidized carbon xerogels (◆), for oxidized carbon xerogels (■) and for Pt/carbon xerogel catalysts synthesized by the Wet Impregnation method (Δ) in a previous study [37].

groups at the surface of the support [22] coupled with an inadequate pH of PTA aqueous solutions during the impregnation step (pH 8.7, i.e. low electrostatic interactions between PTA and the oxidized carbon support cationic Pt complexes and the carbon support, Fig. 2b) provide so many reasons for obtaining of a very low Pt dispersion.

A very important concern regarding Pt/carbon xerogel catalysts is the accessibility of the active centers. Because platinum is located inside the carbon support, there is a risk that it may not be accessible. The values of V_v in Table 2 show that drying under vacuum allows large pore volumes to be retained, but they do not prove the accessibility of platinum. Nevertheless, it can be observed in Table 1 that $d_{\text{TEM}} \cong d_{\text{chem}}$ for all the samples: the mean Pt particle size obtained by CO chemisorption measurements is in each case consistent with TEM measurements. The convergence of TEM and chemisorption measurements tends to indicate that the Pt particles located inside the carbon support are accessible.

Benzene hydrogenation was carried out with samples SEA-550, SEA-625, SEA-550-Ox and SEA-625-Ox to check: (i) whether the very highly dispersed Pt particles located inside the carbon support are accessible for large molecules such as C_6H_6 ; (ii) whether a relationship exists between the high Pt dispersion of Pt/carbon xerogel catalysts and the benzene activity. In previous studies [34–36], it has been observed that benzene hydrogenation is a structure-insensitive reaction on Pt-based catalysts supported on activated carbons. In other words, the reaction rate is directly proportional to the accessible Pt surface (i.e., to the metal dispersion). In Fig. 6, the catalytic activity at 393 K, expressed in mmol of benzene transformed into cyclohexane per unit mass of Pt and per second, r_{ben} , is presented as a function of the Pt dispersion, D_{Pt} for the four samples SEA-550, SEA-625, SEA-550-Ox and SEA-625-Ox and for three Pt/carbon xerogel catalysts synthesized by the Wet Impregnation method (aqueous solution in excess) in a previous study [37]. In Fig. 6, it can be observed for samples SEA-550, SEA-625 and the three Pt/unoxidized carbon xerogels synthesized in [37] that r_{ben} is directly proportional to the Pt dispersion, D_{Pt} , which is consistent with the structure-insensitive nature of the benzene hydrogenation on Pt.

However, samples SEA-550-Ox and SEA-625-Ox, synthesized from oxidized carbon xerogels, are much more active than all the Pt/unoxidized carbon xerogel catalysts. According to previous results for benzene hydrogenation over Pt supported on active carbons [35], better values of r_{ben} (mmol g_{Pt}⁻¹ s⁻¹) are obtained when active carbons are oxidized by nitric acid solutions. In the above-cited study [35], this result is explained by: (i) a better dispersion obtained on the oxidized supports in the considered synthesis conditions; (ii) the significant change in the surface area and pore size distribution after oxidation of the carbon supports. In the

present study, both items are inapplicable: (i) all Pt/C xerogel catalysts synthesized from the SEA method are very highly dispersed ($d_{\text{TEM}} = 1.1\text{--}1.3$ nm in Table 1); (ii) the textural properties of both the unoxidized and oxidized carbon xerogels are very similar (Table 2).

Assuming that the benzene hydrogenation reaction remains structure-insensitive, the fact that the data obtained with SEA-550-Ox and SEA-625-Ox do not fall within the same linear relationship as the other samples (Fig. 6) can be explained in two general ways: (i) a first explanation may be offered in terms of electronic effects. It is well known that the presence of surface functional groups can affect the activity and selectivity of the active phase via metal–support interactions, as previously reported for Pt/C catalysts in selective hydrogenations [46–48]. A remarkable increase in the activity for methanol electrooxidation was also observed when Pt–Ru catalysts were supported on oxidized carbon xerogel [6]. However, the precise nature of this effect has not yet been clearly elucidated. The nature of the metal–support interaction involves a change in the electronic structure of Pt particles, altering the catalytic properties of the Pt surface atoms. For instance, it has been found that the turnover frequency (TOF) of tetralin hydrogenation on zeolite supported Pt catalysts strongly depends on the composition of the support [49]. In the present case, it may be envisaged that the presence of oxygen groups in the vicinity of small Pt crystallites will generate a polarization within the Pt particle, which will lead to a change in the electron affinity of the Pt 5d valence orbitals. This may favor the adsorption of the planar benzene ring. Furthermore, the competition of the carbon support for benzene adsorption will decrease in the presence of oxygen surface groups [50]. Both effects will enhance the catalytic activity of Pt; (ii) a second explanation may be offered by the fact that the metal dispersion of the catalyst calculated from CO chemisorption is not correct. The calculation of D_{Pt} could be distorted by a partial poisoning of the Pt particle surface. Indeed, if the reduction treatment is not sufficient, chlorine atoms coming from the Pt complex could still be present in the catalyst, either on the support or on the Pt particles: chlorine would then block adsorption sites for benzene. Due to the fact that six Cl atoms are contained in one CPA molecule while two Cl atoms are present in one PTA molecule, it seems possible that the chlorine content of Pt catalysts supported on unoxidized carbon xerogels will be higher if the reduction treatment does not eliminate all the chlorine coming from the Pt complex. One can argue that, since the CO chemisorption and TEM results are in good agreement, the values of the dispersion are correct. Indeed in this work, it was assumed [37,38] that the chemisorption mean stoichiometry, that is, the mean number of Pt atoms on which one CO molecule is adsorbed, $X_{\text{Pt-CO}}$, equals to 1.61: lower values of $X_{\text{Pt-CO}}$ would lead to lower dispersions, i.e. to lower accessible Pt surfaces and higher ‘equivalent diameter’ (d_{CO}) values, which would be in agreement with Cl poisoning. Another possibility is the removal of Cl by CO during chemisorption: assuming that $X_{\text{Pt-CO}} = 1.61$ is the right stoichiometry, chemisorption and TEM results would then match, but the true metal dispersion, i.e. the fraction of accessible Pt atoms in the catalyst, would be overestimated by chemisorption. Indeed, during the hydrogenation reaction, Cl poisoning would still block some Pt atoms, decreasing the activity of the catalyst. This would explain why Pt catalysts prepared with CPA (unoxidized supports) would be less active than those obtained with PTA (oxidized supports). In fact, a study is in progress to explain the difference in activity for the hydrogenation of benzene between unoxidized and oxidized carbon xerogels, focusing on Cl poisoning.

5. Conclusions

Highly dispersed Pt/C catalysts were obtained by applying the ‘‘strong electrostatic adsorption’’ method to carbon xerogels. Four supports with various maximal pore sizes (18, 32, 68 and 90 nm) were used and their PZC was determined as being equal to 9.4. These carbon xerogels were also oxidized in nitric acid in order to alter irreversibly their surface and to increase the number of surface acidic groups, with the consequence of a strong decrease of their PZC to 2.4. Unoxidized carbon xerogels placed in solutions at pH values below their PZC become protonated, positively charged and then adsorb platinum anions such as hexachloroplatinate $[\text{PtCl}_6]^{2-}$, while oxidized carbon xerogels placed in solutions at pH values above their PZC become deprotonated, negatively charged and adsorb platinum cations such as platinum tetraammine $[\text{Pt}(\text{NH}_3)_4]^{2+}$. Platinum uptake curves reach a maximum with respect to the pH for each platinum precursor (final pH 2.4–2.5 for CPA on unoxidized carbons and final pH 11.0–11.2 for PTA on oxidized supports). At these maxima, Pt/C catalysts are obtained with platinum loadings of about 8 to 10 wt% for CPA and about 1 to 5 wt% for PTA. Indeed, the present study shows that, in the case of oxidized supports, the amount of adsorbed PTA, and thus the Pt weight loading increases linearly with S_{meso} . These results can be explained by the fact that it is not possible for the large Pt ammine complexes, which are believed to retain two hydration sheaths, to penetrate inside the micropores of carbon xerogels. After the reduction step at 473 K for 1 h, all these Pt/carbon xerogel catalysts preserve a high dispersion and very small platinum particles (1.1–1.3 nm) are observed by TEM. These Pt particles are accessible and the Pt/carbon xerogel catalysts are very active for the hydrogenation of benzene into cyclohexane.

These results obtained by applying the SEA method to prepare very highly dispersed Pt/carbon xerogel catalysts are very encouraging, demonstrating the usefulness of this method for heterogeneous catalysis. Research perspectives are numerous. In particular, a study concerning successive ‘‘strong electrostatic adsorptions’’ to achieve Pt loading up to 20 wt%, while keeping the Pt particle size below 3 nm is in progress. Finally, these Pt/carbon xerogel catalysts are now being tested as PEM fuel cell electrocatalysts for the oxygen reduction reaction.

Acknowledgments

The authors thank the Fonds de Bay, the Fonds de Recherche Fondamentale Collective, the Ministère de la Région Wallonne Direction Générale des Technologies, de la Recherche et de l’Energie and the Interuniversity Attraction Pole (IAP-P6/17) for their financial support. S.L. and N.J. are grateful to the F.R.S.-F.N.R.S. for their postdoctoral research positions. S.L. also acknowledges the Commission for Educational Exchange between The United States of America, Belgium and Luxembourg for its financial help (Fulbright grant) in facilitating her postdoctoral secondment to the Chemical Engineering Department at the University of Illinois at Chicago. We also acknowledge the assistance of Vera Santos in the catalytic tests undertaken in the present study.

References

- [1] H.A. Gasteiger, W. Gu, R. Makharia, M.F. Mathias, B. Sompalli, in: W. Vielstich, A. Lamm, H.A. Gasteiger (Eds.), *Handbook of Fuel Cells—Fundamentals, Technology and Applications*, vol. 3, Wiley, Chichester, 2003, pp. 593–610.
- [2] H.A. Gasteiger, S.S. Kocha, B. Sompalli, F.T. Wagner, *Appl. Catal. B* 56 (2005) 9.
- [3] C. Moreno-Castilla, F.J. Maldonado-Hódar, *Carbon* 43 (2005) 455.
- [4] N. Job, B. Heinrichs, F. Ferauche, F. Noville, J. Marien, J.-P. Pirard, *Catal. Today* 102–103 (2005) 234.
- [5] B. Heinrichs, S. Lambert, N. Job, J.-P. Pirard, in: J.R. Regalbuto (Ed.), *Catalyst Preparation: Science and Engineering*, CRC Press/Taylor & Francis Group, Boca Raton, 2007, p. 163.

- [6] J.L. Figueiredo, M.F.R. Pereira, P. Serp, P. Kalck, P.V. Samant, J.B. Fernandes, *Carbon* 44 (2006) 2516.
- [7] J. Marie, S. Berthon-Fabry, M. Chatenet, E. Chainet, R. Pirard, N. Cornet, *J. Appl. Electrochem.* 37 (2007) 147.
- [8] N. Job, J. Marie, S. Lambert, S. Berthon-Fabry, P. Achard, *Energy Convers. Manage.* 49 (2008) 2461.
- [9] H. Du, B. Li, F. Kang, R. Fu, Y. Zeng, *Carbon* 45 (2007) 429.
- [10] R.W. Pekala, *J. Mater. Sci.* 24 (1989) 3221.
- [11] S.A. Al-Muhtaseb, J.A. Ritter, *Adv. Mater.* 15 (2003) 101.
- [12] N. Job, B. Heinrichs, S. Lambert, J.-F. Colomer, B. Vertruyen, J. Marien, J.-P. Pirard, *AIChE J.* 52 (2006) 2663.
- [13] J.P. Brunelle, *Pure Appl. Chem.* 50 (1978) 1211.
- [14] J.R. Regalbuto, A. Navada, S. Shadid, M.L. Bricker, Q. Chen, *J. Catal.* 184 (1999) 335.
- [15] W.A. Spieker, J.R. Regalbuto, *Stud. Surf. Sci. Catal.* 130 (2000) 203.
- [16] W.A. Spieker, J.R. Regalbuto, *Chem. Eng. Sci.* 56 (2001) 3491.
- [17] X. Hao, J.R. Regalbuto, *J. Colloid Interface Sci.* 267 (2003) 259.
- [18] M. Schreier, J.R. Regalbuto, *J. Catal.* 225 (2004) 190.
- [19] J.T. Miller, M. Schreier, A.J. Kropf, J.R. Regalbuto, *J. Catal.* 225 (2004) 203.
- [20] A. Sepúlveda-Escribano, F. Coloma, F. Rodríguez-Renoso, *Appl. Catal. A* 173 (1998) 247.
- [21] J.L. Figueiredo, M.F. Pereira, M.M.A. Freitas, J.J.M. Orfao, *Carbon* 37 (1999) 1379.
- [22] M.A. Fraga, E. Jordao, M.J. Mendes, M.M.A. Freitas, J.L. Faria, J.L. Figueiredo, *J. Catal.* 209 (2002) 355.
- [23] H.E. van Dam, H. van Bekkum, *J. Catal.* 131 (1991) 335.
- [24] X. Hao, L. Quach, J. Korah, W.A. Spieker, J.R. Regalbuto, *J. Mol. Catal. A* 219 (2004) 97.
- [25] N. Job, R. Pirard, J. Marien, J.-P. Pirard, *Carbon* 42 (2004) 619.
- [26] N. Job, A. Théry, R. Pirard, J. Marien, L. Kocon, J.-N. Rouzaud, F. Béguin, J.-P. Pirard, *Carbon* 43 (2005) 2481.
- [27] J. Park, J.R. Regalbuto, *J. Colloid Interface Sci.* 175 (1995) 239.
- [28] J.R. Regalbuto, in: J.R. Regalbuto (Ed.), *Catalyst Preparation: Science and Engineering*, CRC Press/Taylor & Francis Group, Boca Raton, 2007, p. 297.
- [29] A.J. Lecloux, in: J.R. Anderson, M. Boudart (Eds.), *Catalysis: Science and Technology*, vol. 2, Springer-Verlag, Berlin, 1981, p. 171.
- [30] C. Alié, S. Lambert, B. Heinrichs, J.-P. Pirard, *J. Sol-Gel Sci. Technol.* 26 (2003) 827.
- [31] E.W. Washburn, *Proc. Natl. Acad. Sci. USA* 7 (1921) 115.
- [32] G. Bergeret, P. Gallezot, in: G. Ertl, H. Knözinger, J. Weitkamp (Eds.), *Handbook of Heterogeneous Catalysis*, Wiley-VCH, Weinheim, 1997, p. 439.
- [33] R.J. Farrauto, C.H. Bartholomew, *Fundamentals of Industrial Catalytic Processes*, Blackie Academic & Professionals/Chapman & Hall, London, 1997, p. 436.
- [34] A.E. Aksoylu, M. Madalena, A. Freitas, J.L. Figueiredo, *Appl. Catal. A* 192 (2000) 29.
- [35] A.E. Aksoylu, M. Madalena, A. Freitas, M.F.R. Pereira, J.L. Figueiredo, *Carbon* 39 (2001) 175.
- [36] A.E. Aksoylu, J.L. Faria, M.F.R. Pereira, J.L. Figueiredo, P. Serp, J.-C. Hierso, R. Feurer, Y. Kihn, P. Kalck, *Appl. Catal. A* 243 (2003) 357.
- [37] N. Job, M.F. Ribeiro Pereira, S. Lambert, A. Cabiac, G. Delahay, J.-F. Colomer, J. Marien, J.L. Figueiredo, J.-P. Pirard, *J. Catal.* 240 (2006) 160.
- [38] S.D. Lin, M.A. Vannice, *J. Catal.* 143 (1993) 539.
- [39] C.N. Satterfield, *Mass Transfer in Heterogeneous Catalysis*, MIT Press, Cambridge, 1970.
- [40] P. Vinke, M. van der Eijk, M. Verbree, A.F. Voskamp, H. van Bekkum, *Carbon* 32 (1994) 675.
- [41] N. Santhanam, T.A. Conforti, W. Spieker, J.R. Regalbuto, *Catal. Today* 21 (1994) 141.
- [42] G.C. Torres, E.L. Jablonski, G.T. Baronetti, A.A. Castro, S.R. de Miguel, O.A. Scelza, M.D. Blanco, M.A. Pena Jiménez, J.L.G. Fierro, *Appl. Catal. A* 161 (1997) 213.
- [43] F. Rodríguez-Reinoso, *Carbon* 36 (1998) 159.
- [44] M. Che, O. Clause, C. Marcilly, in: G. Ertl, H. Knözinger, J. Weitkamp (Eds.), *Handbook of Heterogeneous Catalysis*, Wiley-VCH, Weinheim, 1997, p. 191.
- [45] R. Schlögl, in: G. Ertl, H. Knözinger, J. Weitkamp (Eds.), *Handbook of Heterogeneous Catalysis*, Wiley-VCH, Weinheim, 1997, p. 138.
- [46] F. Coloma, A. Sepúlveda-Escribano, F. Rodríguez-Reinoso, *Appl. Catal. A* 150 (1997) 165.
- [47] M.L. Toebes, F.F. Prinsloo, J.H. Bitter, A.J. van Pillel, K.P. de Jong, *J. Catal.* 214 (2003) 78.
- [48] M.L. Toebes, Y. Zhang, J. Hájek, T.A. Nijhuis, J.H. Bitter, A. Jos van Pillel, D.Y. Murzin, D.C. Koningsberger, K.P. de Jong, *J. Catal.* 226 (2004) 215.
- [49] D.E. Ramaker, J. de Graaf, J.A.R. van Veen, D.C. Koningsberger, *J. Catal.* 203 (2001) 7.
- [50] M. Domingo-García, F.J. Lopez-Garzon, M. Perez-Mendoza, *J. Colloid Interface Sci.* 222 (2000) 233.